Journal of Coastal Research	28	3	547–556	West Palm Beach, Florida	May 2012

Tidal Inlet Morphology Classification and Empirical Determination of Seaward and Down-Drift Extents of Tidal Inlets

www.cerf-jcr.org

Erica Carr-Betts[†], **Tanya M. Beck**[‡], **and Nicholas C. Kraus**[‡]

[†]7643 NW 70th Avenue
Parkland, FL 33067, U.S.A.
bettscarr@bellsouth.net

[‡]U.S. Army Engineer Research and Development Center
Coastal and Hydraulics Laboratory
3909 Halls Ferry Road
Vicksburg, MS 39180-6199, U.S.A.

www.JCRonline.org

ABSTRACT

CARR-BETTS, E.; BECK, T.M., and KRAUS, N.C., 2012. Tidal inlet morphology classification and empirical determination of seaward and down-drift extents of tidal inlets. *Journal of Coastal Research,* 28(3), 547–556. West Palm Beach (Florida), ISSN 0749-0208.

The Hayes classification of tidal inlet geomorphic type and the distances from the inlet to the most seaward and down-drift extents of ebb deltas are examined. For this purpose, a database was compiled for 89 tidal inlets along the Atlantic Ocean, Gulf of Mexico, and Pacific Ocean coasts of the United States. The database contains spring or diurnal tidal prism and the average significant wave height and wave period from a 20-year hindcast. The Hayes diagram aims to classify inlet plan-view morphology by tide range and wave height. Based on the work presented here, it is concluded that the inlet classification of Hayes has limited applicability for describing the morphology of typical tidal inlets, and replacement of tide range by inlet tidal prism did not improve the classification. Best correlation for the two ebb delta extents was found for inlets segregated by wave exposure (as mild, moderate, or high) and by tidal prism. There was poor or no correlation for moderately wave-exposed inlets, and moderate to high correlation was found for mildly and highly exposed inlets. The seaward and down-drift extents of inlets tend to remain constant up to a tidal prism less than 10^8 m^3, depending on wave exposure, and then increase linearly with tidal prism. It is postulated that a tidal prism less than approximately 10^8 m^3 is a tipping point required to overcome other factors controlling tidal inlet plan-form morphology.

ADDITIONAL INDEX WORDS: *Tidal inlet, tidal prism, tidal inlet morphology, tide dominated, wave dominated, mixed energy inlets.*

INTRODUCTION

Most studies of tidal inlets refer to the classification of Hayes (1979) to place the site into a geomorphic context. A tidal inlet is an opening in the shore that allows exchange of water between the ocean and bays, lagoons, and marsh and tidal creek systems, and for which the tidal current maintains the main channel of the inlet (FitzGerald, 2005). The Hayes (1979) classification is aimed to identify geomorphic inlet type by tide range and mean wave height, and it has limiting states of tide-dominated and wave-dominated, with mixed states defined in between. The classification thus attempts to convey qualitative information about the plan-view geomorphology of a tidal inlet. Wave-dominated inlets are understood to have ebb deltas that are smaller in area and volume than tide-dominated inlets and are typically associated with microtidal ranges (range < 2 m, according to Davies [1964]), whereas tide-dominated coasts have well-developed ebb deltas and are typically associated with meso-tidal ranges (2 m $<$ range $<$ 4 m). In their 1984 paper Davis and Hayes (1984) also examine additional variables to describe the plan-view geomorphology of a tidal inlet. Ebb deltas at wave-dominated tidal inlets typically have arcuate or horseshoe-shaped bypassing bars and a shoal in front of the ebb jet (the "ebb delta proper" following the terminology of Kraus [2000]), and tide-dominated inlets tend to exhibit two shore-normal parallel channel margin bars, without an ebb delta proper. Because mixed-energy inlets can exhibit a wide range of varying energy forcing (both wave and tidal), their ebb deltas are not as easily defined and may exhibit a variety of morphologies (FitzGerald, 1982). Typical morphologic features associated with mixed-energy ebb deltas include an updrift channel margin-linear bar, a flood marginal channel along the updrift side of the delta, and a large and shallow bypassing platform along the downdrift side of the delta.

Bruun and Gerritsen (1959) identified two mechanisms for natural sediment bypassing at tidal inlets: (1) wave-induced sand transport along the periphery of the ebb delta (bar bypassing), most applicable to wave-dominated inlets, (2) transport of sand in channels by tidal currents (tidal bypassing), most applicable at tide-dominated inlets. FitzGerald (1982) examined sediment bypassing at nonstructured, mixed energy tide-dominated inlets and identified a discontinuous or episodic process of attachment of portions of the ebb delta to the downdrift shore (see Gaudiano and Kana [2000] for a case study). Such detachment or significant shoal migration as a

DOI: 10.2112/JCOASTRES-D-11-00124.1 received 10 July 2011; accepted in revision 27 September 2011.
Published Pre-print online 5 January 2012.
© Coastal Education & Research Foundation 2012.

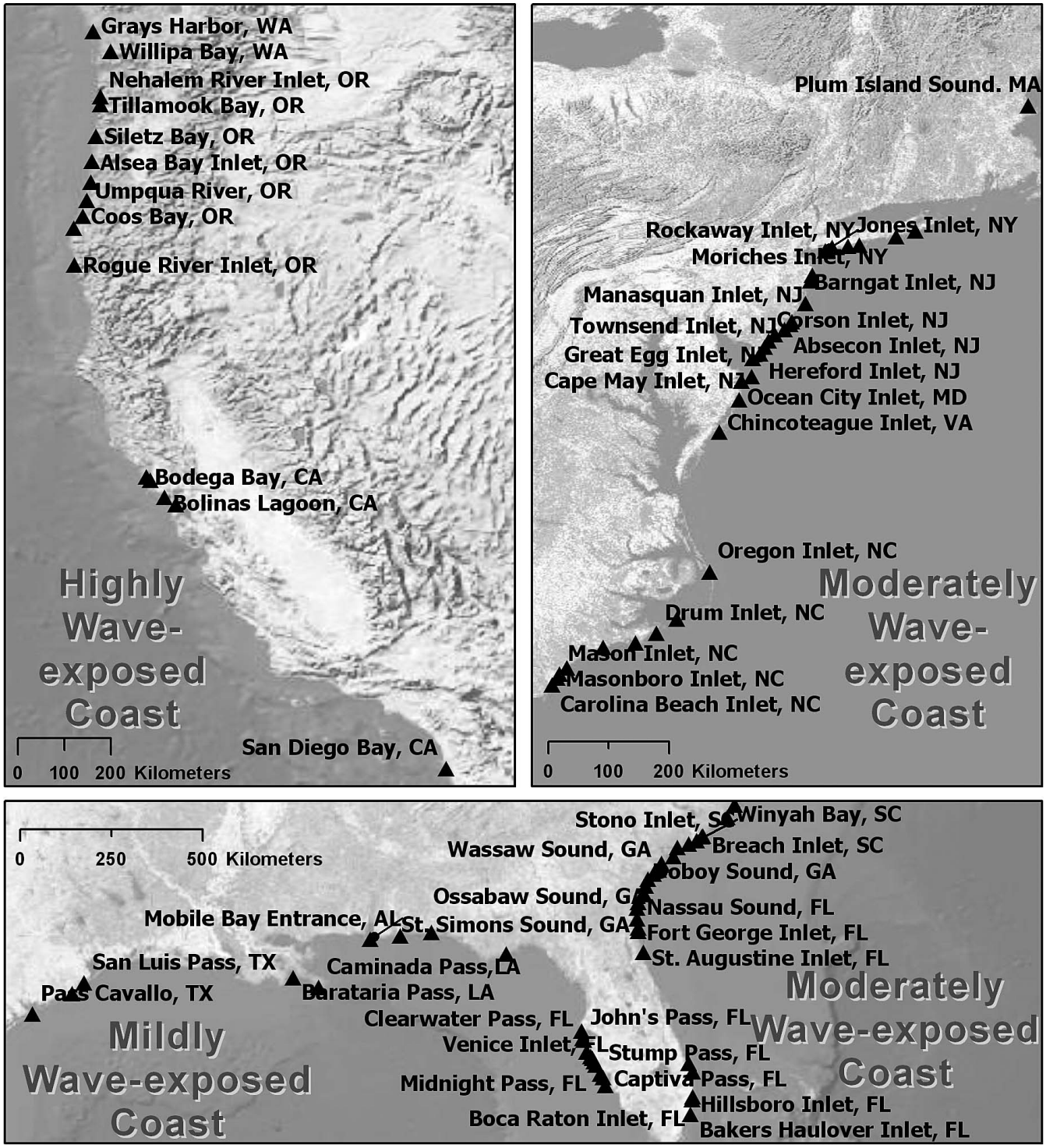

Figure 1. A map of the 89 inlets examined along the three wave energy exposure U.S. coasts with the associated exposure ranges as described by Walton and Adams (1976).

collective feature (Sonu, 1968) is also manifested in structured inlets as jetty tip shoals, sand bodies that migrate around, typically, the updrift jetty to deposit near or in the navigation channel. For design and management of inlets, especially those inlets stabilized by jetties and those to be dredged for navigation, a general classification scheme of inlets according to their wave environment, if valid, provides helpful information for both initial desk-top planning and in

Figure 2. Examples of inlet type classified by inspection of aerial photographs in this study. (A) Tide-dominated inlet, Boca Grande Inlet, Florida; (B) Mixed energy (structured), Masonboro Inlet, North Carolina; (C) Mixed-energy inlet (without jetties), New Pass, Florida; and (D) Wave-dominated stabilized inlet: Shinnecock Inlet, New York.

subsequent quantitative analysis. However, site experiences have revealed tidal inlets (structured and unstructured) that did not fall into the expected classification, motivating the present study.

This study was conducted to increase the range of tidal inlets previously examined for dominant morphologic type. Based on inlet type, wave exposure according to Walton and Adams (1976), and tidal prism, quantitative information was empirically obtained for two geomorphic descriptors: the greatest seaward extent of the ebb delta and the distance from the inlet to the downdrift attachment bar. Tidal prism is the volume of water entering an inlet at flood tide or exiting on ebb tide, taken here as during the spring or diurnal maximum tide and excluding contributions from freshwater flow. Both structured (stabilized by jetties) and unstructured inlets were covered in this analysis.

DATABASE AND PROCEDURE

Eighty-nine inlets along the Atlantic, Pacific, and Gulf of Mexico coasts of the United States were examined to assess their compatibility with the Hayes (1979) diagram and to develop empirical relationships between the seaward and downdrift extents of their ebb deltas and the local hydraulic forcing parameters (mean tidal range, mean significant wave height, mean wave period, and tidal prism). A range of information sources was accessed to assemble and cross-check the tidal inlet forcing parameters, including inlet management plans, industry reports, and personal communications with coastal engineering professionals conducting studies at various tidal inlets. These sources are, in many cases, the entities responsible for previous data collection and management at the inlet. The analysis included some aerial photographs assembled by Vincent and Corson (1981), who examined 67 tidal inlets in the United States to determine six geomorphic parameters of tidal inlets. Figure 1 illustrates all of the 89 inlets examined along the three wave-energy exposure U.S. coasts with the associated exposure ranges as described by Walton and Adams (1976). An explanation of this is provided further in this article. A figure of tidal ranges along the United States is presented in Davies (1964).

Following concepts and methods in Hayes (1979), the inlets were separated into three morphologic classes (wave-dominated, tide-dominated, and mixed-energy) based on inspection of aerial imagery and nautical charts produced by the National Oceanic and Atmospheric Administration, National Ocean Service (NOS). As an example of the Hayes (1979) conception of the three morphologic classes, ebb-tidal deltas were identified as having zero, one, or two channel margin-linear bars extending along the main ebb channel and indicating wave-to-mixed energy dominance, mixed-energy, and tide-dominated, respectively. Additionally, the shape of the ebb delta and the presence of flood-tidal deltas further clarified wave or tidal dominance. Fifty-seven inlets were classified as wave-dominated, nine inlets were classified as tide-dominated, and twenty-three inlets were classified as mixed energy. Figure 2 gives examples of an inlet morphologic type determined from ebb delta morphology, as evident in aerial photographs, and to illustrate the authors' decision process. In Figure 2, (A) is Boca Grande Inlet, Florida, exhibiting a tide-dominated morphology with large marginal-linear shoals extending along the channel; (B) is Masonboro Inlet, North Carolina, exhibiting a mixed-energy morphology with jetties; (C) is New Pass, Florida, exhibiting a natural mixed-energy morphology with one updrift channel margin linear bar and a large downdrift bypassing platform; and (D) is Shinnecock Inlet, New York, exhibiting a wave-dominated inlet with a large arcuate bypassing bar characterizing the ebb delta.

Forcing Parameters

Mean significant wave height and the associated mean peak-wave period were obtained for the 89 inlets from 20-year hindcast statistics (U.S. Army Corps of Engineers, 2010).

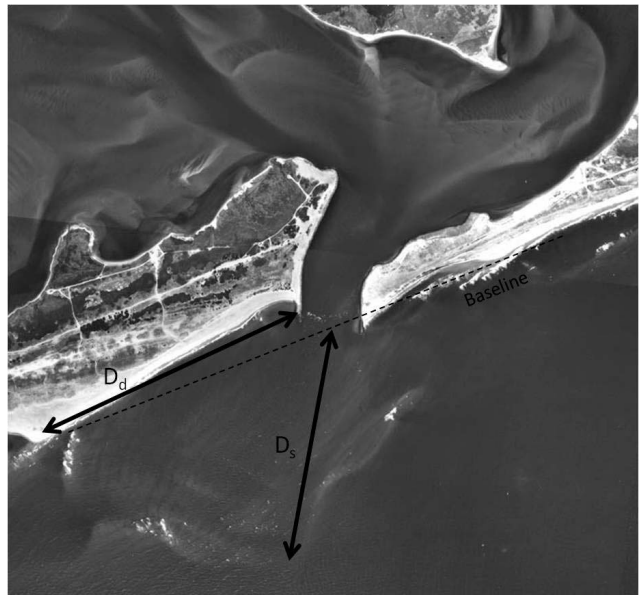

Figure 3. Definition of most seaward extent of ebb delta D_s and the distance to the downdrift attachment bar D_d. Moriches Inlet, New York. Date: 20 March 1995.

Although wave hindcasts have limitations, this procedure is expected to provide uniformity for the needed wave information around the coast of the United States. Tide range was obtained from the closest NOS sea-tide gauge (NOAA NOS, 2010). Tidal prism was compiled from Jarrett (1976), inlet management plans, and other sources. The tidal inlet database compiled for the present study is available on the Coastal Inlets Research Program (CIRP) website (U.S. Army Corps of Engineers, 2011).

Tidal prism (P) has been found to be a key predictor of many morphologic features of tidal deltas, such as minimum channel cross section (Jarrett, 1976), volume of ebb deltas (Carr-Betts, 2002; Marino and Mehta, 1987; Walton and Adams, 1976), and volume of flood deltas (Carr de Betts, 1999). A review by Kraus (2009) gives other predictive relations for morphologic descriptors of inlets related to tidal prism. Because of the expected predictive capability of tidal prisms for inlet morphology, only inlets with measured or calculated tidal prisms were included in the database.

Walton and Adams (1976) introduced the parameter H^2T^2, where H is mean wave height (here, taken to be the mean significant wave height), and T is wave period, to define mildly wave-exposed (0–2.8 m^2s^2), moderately wave-exposed (2.8–27.9 m^2s^2), and highly wave-exposed coastlines (>27.9 m^2s^2). Their analysis of 44 U.S. inlets placed South Carolina, Texas, and the lower Gulf Coast of Florida inlets into the mildly wave-exposed range; the Atlantic coast and Panhandle of Florida on the Gulf Coast into the moderately wave-exposed range; and the Pacific coast inlets into the highly wave-exposed range. In this article we utilized the parameter H^2T^2 to assess potential correlations between dependent and independent variables.

Response Parameters

Aerial photographs and nautical charts were analyzed to evaluate the seaward and downdrift longshore extents of ebb tidal deltas. Unrectified aerial photographs of different scales were consulted, with individual photograph scales determined through comparison of distance between two stationary objects, such as two jetties. On some photographs the ebb delta could be identified through calm water. For other photographs the location of the ebb delta had to be inferred by wave refraction and diffraction patterns (Gibeaut and Davis, 1993). Uncertainty is associated with the latter situation. If the ebb delta could not be readily identified, the photograph was eliminated from analysis. For some Pacific coast and highly wave-exposed Atlantic coasts, the location of the breaking waves for fair-weather waves is located landward of the terminal lobe of the ebb delta (due to their great depths), and therefore nautical charts were necessary for analysis.

Two geometric properties of the ebb-delta plan view shapes were obtained from interpreting the photographs (Figure 3) or nautical charts: the distance to the most seaward extent of the ebb delta D_s and the distance to the down-drift attachment bar D_d. The quantities D_s and D_d were measureable for 88 and 86 inlets, respectively, of the 89 inlets in the database. Although measurements were made from one source for each inlet (most recent aerial photograph or nautical chart), several sources were reviewed for the inlet to ensure the determination was reliable. Uncertainties introduced for the distance measurements are estimated to be 25 to 150 m, depending on the scale, distortion, and parallax on the aerial photograph. Inlets selected for analysis were considered mature and assumed to be in equilibrium. The volume of river flow associated with tidal inlets and the seasonality of this flow has not been taken into account in this article. The authors are presently including this information within the CIRP inlets database and anticipate future research to include the effects of river flow on tidal inlet morphology.

The distance to the most seaward extent of the ebb delta D_s was measured along a straight baseline set parallel to the trend of the shoreline. The measurement began at the channel centerline along the baseline and extended to the terminus of the ebb delta. Additional information regarding how the distance was measured may be found in Carr and Kraus (2001). In aerial photographs this distance was determined visually based on the identification of the ebb delta through tonal changes (Gibeaut and Davis, 1993). Nautical charts were analyzed if aerial photographs were not available or if ebb delta plan views were not distinguishable on photographs, e.g., at Pacific coast inlets with greater ebb shoal extents. Distance to the seaward extent of the ebb delta on nautical charts was determined as the point at which the contour lines were oriented similar to offshore contours far from the inlet (Vincent and Corson, 1981). This distance was visually clear and easily identified by assessment of the slopes at the terminal lobe of the ebb delta. Gentle contours were identified over the ebb delta, transitioning to greater slopes as the ebb delta met the continental shelf.

A consistent interpretation of the location of the shoreline from the aerial photographs and nautical charts was attempted. A baseline was determined with two end points located at the updrift and downdrift shorelines outside of the direct influence of the inlet or terminal structures. This methodology is similar to that of Gibeaut and Davis (1993), whose baseline end points were located where the ebb delta intersected the shoreline to obtain a shoreline trend from which their measurements could commence. Figure 3 shows an example of the shoreline trend utilized for measurement of the distance to the most seaward extent of the ebb delta. The identification of a baseline from which measurements are taken effectively eliminates ambiguity of an updrift and downdrift shoreline offset. For example, Grays Harbor, Washington, has a large shoreline offset (approximately 3 km), whereas Mason Inlet, North Carolina, has negligible offset. Shoreline offsets may be produced by coastal structures adjacent to the jetty or from the presence of the ebb delta attachment.

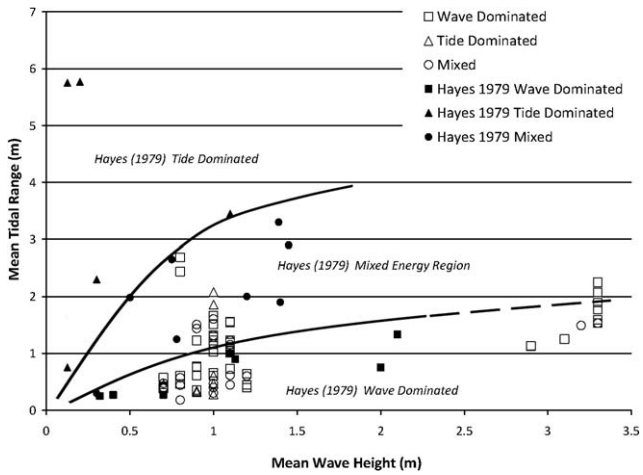

Figure 4. Augmented Hayes (1979) diagram plotting 20 of his original 21 inlets and 89 additional inlets. Mixed-energy tide-dominated and mixed-energy wave-dominated classifications of the Hayes diagram are omitted. Original Hayes diagram lines covered mean wave heights to about 1.5 m for tide-dominated inlets and 2.5 m for wave-dominated inlets (solid lines). The dashed line indicates extension of the trend for this study.

The distance to the downdrift attachment bar D_d was measured along a straight baseline set parallel to the trend of the shoreline. The measurement began at the downdrift inlet shoreline (at the narrowest section of the inlet channel) and ended at the location of the ebb delta attachment to the downdrift shoreline (Figure 3). If the location of the narrowest section of the inlet channel was not located along the baseline, then the measurement origin was translated perpendicularly to begin along the baseline. An attempt was made to determine a distance to the updrift attachment bar, as done by Carr and Kraus (2001), for a limited number of inlets, but identification was difficult at most of the additional inlets examined. Updrift bypassing bars were found to be rare at inlets stabilized by jetties, so this parameter was not analyzed.

RESULTS

One hundred and five empirical associations of various types were attempted between potential forcing and geomorphic

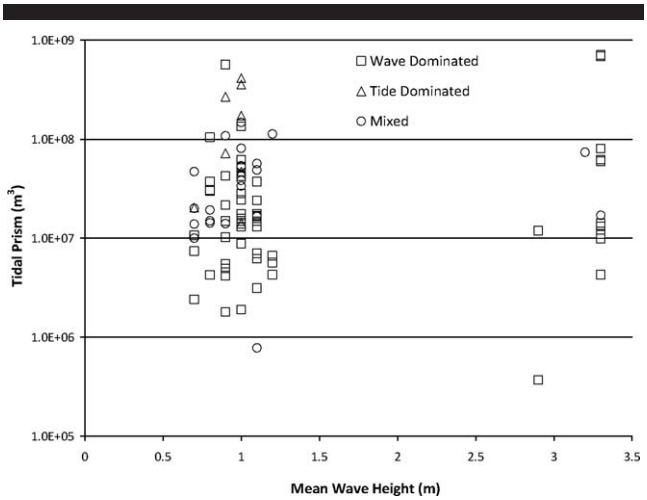

Figure 5. Inlet morphology type plotted with tidal prism and mean wave height. No classification of morphology type is apparent.

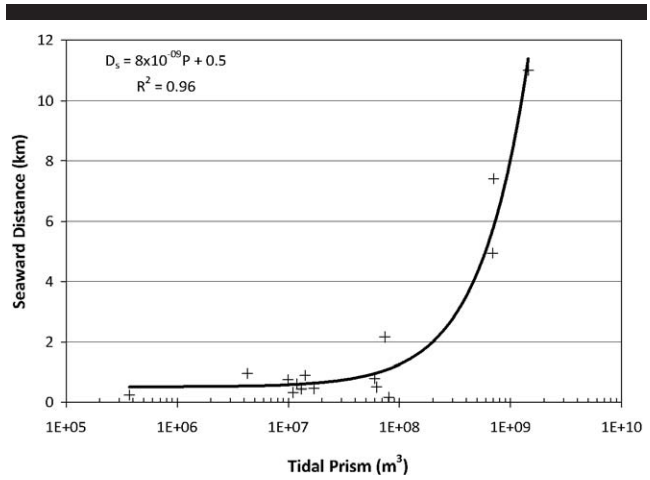

Figure 7. D_s *vs.* P for 15 highly wave-exposed inlets. The best fit is D_s (km) = $8 \times 10^{-9}P + 0.5$.

response parameters. The associations examined a broad range of forcing parameters including (1) tidal prism, (2) tidal prism and wave-height combination as considered by Buonaiuto and Kraus (2003), (3) combination of tidal prism and width of the inlet, (4) the Walton and Adams (1976) parameter classifying wave-energy exposure regime and location of the inlet as on Atlantic, Gulf, or Pacific coast, (5) number of jetties (as zero, one, or two), and the responses of D_s and D_d. The most successful correlations were the tidal prism and wave-exposure parameter of Walton and Adams (1976), and these correlations are presented here.

Augmented Hayes Diagram

The 89 data points assembled are plotted in Figure 4 together with 20 of the 21 original points of Hayes (1979) that could be identified by the authors. Hayes included five classifications of geomorphic inlet type-based on the tide range and wave height. However, in this research, based on lack of segregation of the data, there appears to be no justification for a classification describing mixed-energy tide-dominated and mixed-energy wave-dominated inlets. There is little separation of the tidal inlet morphologic type based on mean tide range, with three inlets clearly classified by visual inspection as wave-dominated (Plum Island Sound, Essex Bay Inlet, and Newbury Port Harbor, all in Massachusetts) but lying close to the original line demarking tide-dominated. Many inlets classified visually as tide-dominated fall into the Hayes category of wave-dominated (for example, New Pass, Lee County, Redfish Pass, Boca Grande Pass, Pensacola Bay Entrance, and Bunces Pass, all in Florida; and Barataria Pass, Louisiana).

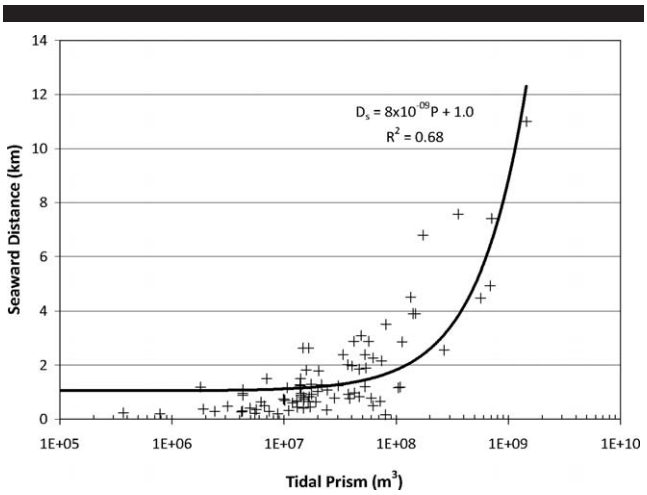

Figure 6. D_s *vs.* P for 88 inlets in the database. The best fit is D_s (km) = $8 \times 10^{-9}P + 1.0$.

The inlets presented in the original Hayes (1979) diagram were not typical barrier island inlets. Some of them were fjords, and Bristol Bay and the Copper River Delta in Alaska included in the original diagram may not be considered as tidal inlets (based upon the definition that the main inlet channel be maintained by the tidal current [FitzGerald, 2005]) but rather as entrances to large bays. The Bay of Fundy, included in the original Hayes diagram, is an entrance with an extremely large tidal range and a small mean wave height. Such sites differ from the more typical and less extreme barrier-inlet systems examined in the present study. This may explain why, in the original study by Hayes (1979), the classification did seem to work.

It is concluded that, except for extremes of either tide range or wave height, the inlet classification approach of Hayes (1979) holds little utility. This finding extends the observations of Davis and Hayes (1984), who discuss other variables that might determine or limit the end state of inlet morphology, including physiography and stratigraphic sequences. They hypothesized that tidal prism, instead of tidal range, would provide improved prediction of inlet morphology type, stating, "Exceptions to these stated generalizations are so numerous that wave energy and tidal prism must be included in characterizing coasts. It is possible to have wave-dominated coasts with virtually any tidal range and likewise possible to

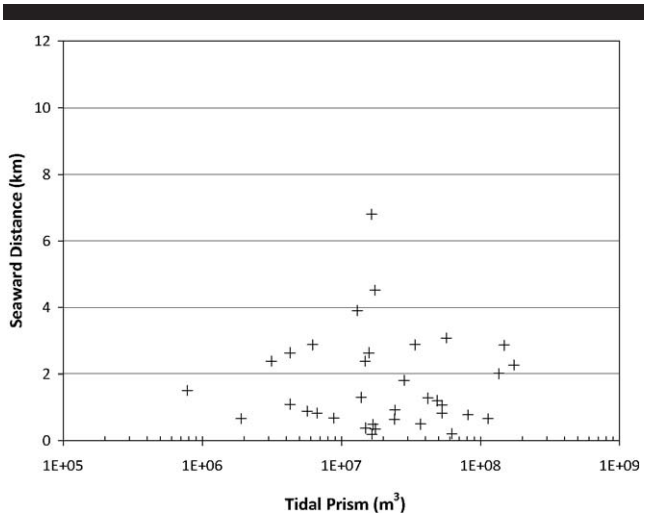

Figure 8. D_s *vs.* P for 38 moderately wave-exposed inlets. No correlation is evident between D_s and tidal prism.

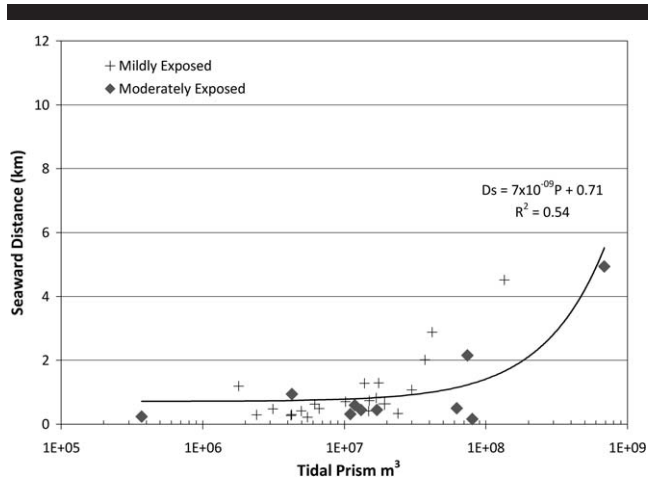

Figure 10. D_s *vs.* P for 30 dual-jettied inlets. The best fit is D_s (km) = $7 \times 10^{-9}P + 0.7$.

have tide-dominated coasts even with very small (tide) ranges" (p. 313). However, Figure 5 plots the classification data against tidal prism and mean wave height, and no segregation of inlet morphologic type with tidal prism in lieu of tide range is found. It is of note that the wave heights were taken directly from the graphic presented in the Hayes (1979) paper and that the sources of this data are unknown to the authors of the present paper. The authors attempted to reproduce the data given in the Hayes paper which utilized mean wave height and wave height data available from WIS (mean significant wave height) given data constraints. Ongoing research may be able to address the inconsistencies in wave height source to a greater extent.

Seaward Extent of Ebb Delta, D_s

The seaward extent of an ebb delta is expected to be proportional to the magnitude of the tidal prism, based on experience with many inlet morphologic properties that correlate with prism (as summarized by Kraus [2009]). Figure 6 plots the results for all inlets, and Figures 7 through 9 plot results for highly, moderately, and mildly wave-exposed coasts as defined by Walton and Adams (1976). Except for the moderately wave-exposed coasts, a visually drawn line for Figure 6 describes the data as $D_s \approx 1$ km for tidal prism with a range less than 10^8 m^3, after which the line of correlation arcs upward exponentially with tidal prism, P, indicating a notable change in behavior of the ebb delta for prism greater than 10^8 m^3. The same general behavior holds true for Figures 7 and 9, with near-constant D_s for $P < 10^8$ m^3. Evidently, there is a tipping point in tidal prism above which it dominates over other possible controlling factors such as wave direction, back-bay configuration, and tidal inlet channel alignment that can contribute to determination of inlet plan-form morphology. Best-fit lines are plotted on Figures 6, 7, and 9 along with their associated equation and correlation coefficient. No correlation between D_s and tidal prism was found for moderately wave-exposed inlets (Figure 8).

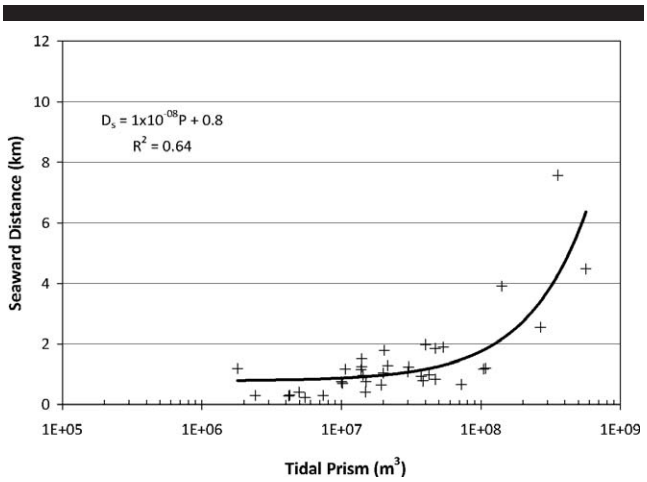

Figure 9. D_s *vs.* P for 36 mildly wave-exposed inlets. The best fit is D_s (km) = $1 \times 10^{-8}P + 0.8$.

In an attempt to understand more fully the predictive relationships being developed in this research, the factors contributing to the observed tipping point tidal prism of 10^8 m^3 were examined in more detail for the case which included all of the inlets. When the inlets with tidal prisms lower than 10^8 m^3 were removed from the remaining inlets no clear relationship with distance to the most seaward extent of the ebb shoal was evident. For the inlets with tidal prisms greater than 10^8, the correlation was only mildly less than that when all the data points were examined. It is hypothesized that the tidal prism larger than a certain value, possibly 10^8 m^3, is necessary to sustain active deposition on the ebb delta beyond one kilometer from the shoreline.

A stronger correlation of D_s and tidal prism was expected for highly wave-exposed inlets because greater wave energy limits the extent to which the ebb delta can grow offshore under a given tidal prism forcing. Many other factors that may contribute to the resultant geometric shape of ebb deltas

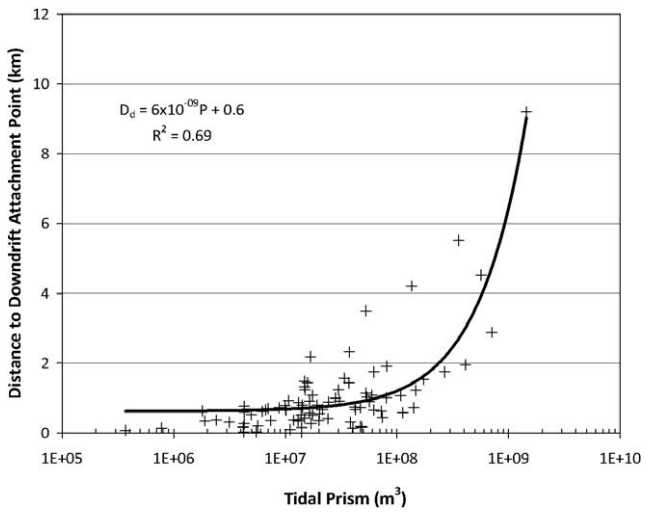

Figure 11. D_d *vs.* P for 86 inlets in the database. The best fit is D_d (km) = $6 \times 10^{-9}P + 0.6$.

include gross sediment transport rates, sediment availability, and the seasonal nature of higher wave energy. It is hypothesized that the poor correlation for moderately wave-exposed inlets is not because they experience a higher wave or tidal forcing, but rather that they are influenced by more variability in forcing types and have similar magnitudes of wave and tidal forcing. Mildly wave-exposed inlets with large tidal prisms are typically situated along wide continental shelves (which gradually dissipate wave energy) and tend to have a shallow offshore platform, for example, as that found at Boca Grande Pass, Florida, and Sapelo Sound Inlet, Georgia. At such sites, the distance to the furthest seaward extent of the ebb delta may be a function of the accommodation space on the shelf and the greater tidal prism. At other inlets, such as Stono Inlet, South Carolina, and Willapa Bay Inlet, Washington, another

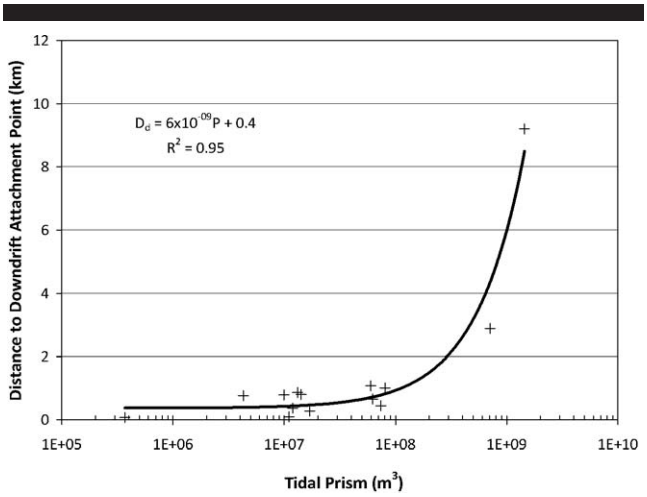

Figure 12. D_d *vs.* P for 15 highly wave-exposed inlets. The best fit is D_d (km) = $6 \times 10^{-9}P + 0.4$.

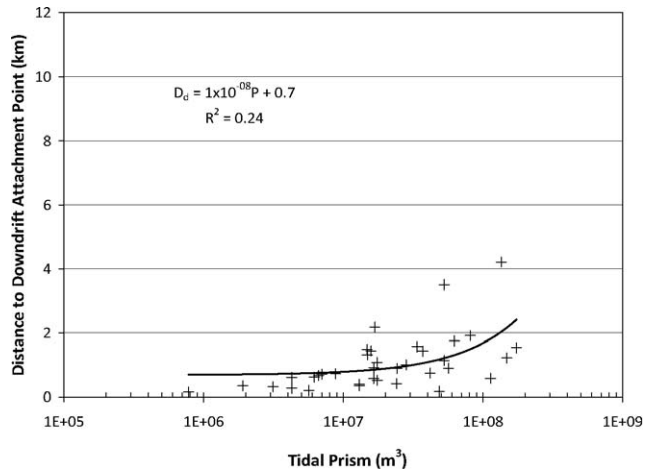

Figure 13. D_d *vs.* P for 38 moderately wave-exposed inlets. The best fit is D_d (km) = $1 \times 10^{-8}P + 0.7$, with weak correlation.

controlling factor to D_s is the amount of available sediment to form large ebb deltas.

Jetties constrict the ebb flow of an inlet, or its ebb jet, and are expected to cause sediment deposition further offshore than a natural inlet with the same tidal prism. Therefore, it was initially hypothesized that the seaward margin of the ebb delta at dual-jettied inlets would be located further offshore. Figure 10 does not indicate a correlation describing this pattern. As an example, the greatest seaward extent of an ebb delta with two jetties was 5 km, and yet the greatest seaward extent of all the inlets (Figure 6) was 11 km for San Francisco Inlet (no jetties). The ebb deltas with the greatest seaward extents were associated with inlets without jetties, which are large tidal inlets for which jetties are neither feasible to construct nor necessary (Mobile Bay Entrance, Alabama; Sapelo Sound Inlet, Georgia; and Willapa Bay Inlet, Washington).

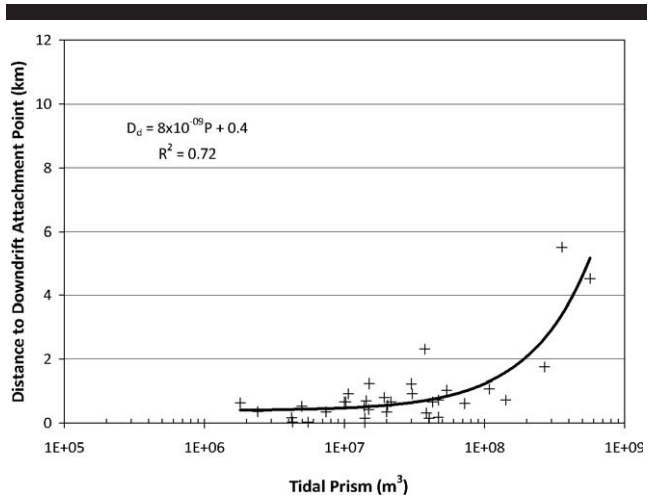

Figure 14. D_d *vs.* P for 34 mildly wave-exposed inlets. The best fit is D_d (km) = $8 \times 10^{-9}P + 0.4$.

Distance to Downdrift Attachment Bar, D_d

Bruun (1995) discussed what he termed the "short" distance and "long" distance of shoreline recession at littoral barriers. The beach segment between the downdrift jetty of an inlet and its attachment bar represents the short distance and has been referred to as an "isolated" beach (Hanson and Kraus, 2001). Longshore sediment-transport input is limited to the isolated beach by the jetty and by the attachment bar, which acts as a groin, and such beaches experience chronic erosion. Further down drift, the long-term influence of the littoral barrier is manifested as a smaller rate of shoreline recession.

The distance to the down-drift attachment bar is, therefore, of great interest in defining the extent of the isolated beach and understanding the scale of coastal change of an inlet. This distance is represented by the quantity D_d. Figure 11 plots the results for all inlets, and Figures 12 through 14 plot results for highly, moderately, and mildly wave-exposed coasts. Similar to the findings in the previous section for D_s, the distance D_d remains approximately constant for tidal prism $P < 10^8$ m^3, then increase linearly with P above this critical value. Trend lines are plotted on Figures 11 through 14 along with their associated equation and correlation coefficient.

A similar analysis of the tipping point tidal prism was performed for the distance to the down-drift attachment bar parameter D_d, for the all inlets case. As in the distance seaward case, minimal correlation for a trend-line developed for data with tidal prisms below the tipping point was observed. A correlation less than but similar to the nonseparated case was observed for inlets with tidal prisms above the tipping point.

As suggested by Bruun (1995), D_d is a characteristic parameter indicating the relative influence of wave and tidal energy forming the bypassing pathways and the associated down-drift attachment. In separating the amount of wave exposure, a reasonable correlation between D_d and tidal prism is found for highly and mildly wave-exposed inlets (Figures 12 and 14), with R^2 of 0.95 and 0.72, respectively. However, moderately wave-exposed inlets exhibit weak correlation between D_d and P (Figure 13). A strong correlation of D_d and P was expected for highly wave-exposed inlets, similarly to D_s, because higher wave energy will modify the lateral extent of sediment bypassing pathways. It is not clear how the lateral extent of sediment transport is modified by tidal processes; it is speculated that the persistent higher wave energy, with greater refraction by large wave periods, dominates the morphology of the inlets through reducing the variation in directional wave exposure.

CONCLUSIONS

A database covering 89 inlets on the Atlantic, Gulf, and Pacific coasts of the United States was compiled and analyzed for conformance with the Hayes (1979) morphologic classification based on average tide range and wave height and to develop empirical predictions for the most seaward extent of the ebb shoal D_s and distance to the downdrift attachment bar D_d.

(1) It is concluded that the Hayes (1979) diagram has limited predictive capability for describing the plan-form morphology of tidal inlets such as exist within barrier islands. Tidal range was replaced by inlet-specific tidal prism in an effort to improve predictive power, but without success.

A number of parameters were examined and inlets were classified (i.e., H^2T^2, $PW_c^{1/4}P^{1/3}$, east, west, or Gulf Coast; mild, moderate, or highly exposed inlets; tide-dominated, wave-dominated, or mixed-energy inlets; number of jetties and combinations of these) to assess potential correlations. Of the many means examined to predict the distances D_s and D_d, it was found that the wave-energy exposure concept of Walton and Adams (1976) and tidal prism had the most predictive power.

(2) The inlets examined tended to have constant distances D_s, and D_d for tidal prisms of $P < 10^8$ m^3, with their values depending on degree of wave exposure, and after which D_s and D_d increased linearly with tidal prism. It is postulated that a tidal prism of about 10^8 m^3 is a tipping point necessary to overcome other factors controlling inlet morphology, such as the difference in net and gross longshore sediment transport, back-bay configuration, and orientation of the inlet main channel.

ACKNOWLEDGMENTS

This study was conducted as an activity of the Inlet Geomorphology Evolution Work Unit of the Coastal Inlets Research Program, a Navigation Research Program of the U.S. Army Corps of Engineers. Work was conducted at the U.S Army Engineer Research and Development Center, Coastal and Hydraulics Laboratory. A draft of this paper benefitted from a review by Douglas Mann, P.E. Coastal Planning & Engineering, Inc., and by Mr. William Seabergh and Dr. Jeffrey Waters, U.S. Army Engineer Research and Development Center, Coastal and Hydraulics Laboratory. Permission was granted by Headquarters, U.S. Army Corps of Engineers, to publish this information. The authors would also like to acknowledge the life and work of Dr. Nicholas Kraus who was a mentor and a friend. Nick is dearly missed by his coauthors and by inlets and their ebb shoals everywhere.

LITERATURE CITED

Bruun, P. and Gerritsen, F., 1959. Natural by-passing of sand at coastal inlets. *Journal of the Waterways and Harbors Division WW4*, 75–107.

Bruun, P., 1995. The development of downdrift erosion. *Journal of Coastal Research*, 11(4), 1242–1257.

Buonaiuto, F.S. and Kraus, N.C., 2003. Limiting slopes and depths at ebb-tidal shoals. *Coastal Engineering*, 48(1), 51–65.

Carr, E.E. and Kraus, N.C., 2001. Morphologic asymmetries at entrances to tidal inlets. *Coastal and Hydraulic Engineering Technical Note ERDC/CHL CHETN-IV-33*. U.S. Army Engineer Research and Development Center, Vicksburg, MS, 16p. http://chl.wes.army.mil/library/publications/chetn.

Carr-Betts, E.E., 2002. Morphologic Asymmetry of Ebb Deltas at Tidal Inlets. Gainesville, Florida: University of Florida, Master's thesis, Report Number UFL/COEL-2002/16, 171p.

Carr de Betts, E.E., 1999. An Examination of Flood Deltas at Florida's Tidal Inlets. Gainesville, Florida: University of Florida, Master's thesis, 125p.

Davies, J.L., 1964. A morphogenic approach to world shorelines. *Zeitschrift für Geomorphologie*, 8, 27–42.

Davis, Jr, R.A. and Hayes, M.O., 1984. What is a wave dominated coast? *Marine Geology*, 60, 313–329.

FitzGerald, D.M., 1982. Sediment bypassing at mixed energy tidal inlets. Reprinted from *Proceedings of the Eighteenth Coastal Engineering Conference*, ASCEI Cape Town, South Africa, November 14–19, 1982), pp. 1094–1118.

FitzGerald, D.M., 2005. Tidal inlets. *In:* Schwartz, M. (ed.), *Encyclopedia of Coastal Science*. New York: Springer, pp. 958–685.

Gaudiano, D.J. and Kana, T.W., 2000. Shoal bypassing in South Carolina tidal inlets: geomorphic variables and empirical predictions for nine mesoscale inlets. *Journal of Coastal Research*, 17(2), 280–291.

Gibeaut, J.C. and Davis, R.A., 1993. Statistical geomorphic classification of ebb-tidal deltas along the west-central Florida coast. *Journal of Coastal Research*, SI(18), 165–184.

Hanson, H. and Kraus, N.C., 2001. Chronic beach erosion adjacent to inlets and remediation by composite (T-head) groins. Coastal Engineering Technical Note CHETN-IV-36, U.S. Army Engineer Research and Development Center, Vicksburg, MS, 15p.

Hayes, M.O., 1979. Barrier island morphology as a function of tidal and wave regime. *In:* Leatherman, S. P (ed.), *Barrier Islands form the Gulf of St. Lawrence to the Gulf of Mexico*. New York: Academic Press, pp. 1–27.

Jarrett, J.T., 1976. Tidal prism—inlet area relationships. GITI Report 3, U.S. Army Engineer Waterways Experiment Station, Vicksburg, MS, 55p.

Kraus, N.C., 2000. Reservoir model of ebb-tidal delta evolution and sand bypassing. *Journal of Waterway, Port, Coastal, and Ocean Engineering*, 126(3), 305–313.

Kraus, N.C., 2009. Engineering of tidal inlets and morphologic consequences. *In:* Kim, Y. (ed.), *Handbook of Coastal Engineering*, Chapter 31. Hackensack, New Jersey: World Scientific Publishing, pp. 867–900.

Marino, J.N. and Mehta, A.J., 1987. Inlet ebb tide shoals related to coastal parameters. *In: Proceedings Coastal Sediments 87* (Reston, Virginia: ASCE Press), pp. 1608–1622.

National Oceanic and Atmospheric Administration, National Ocean Service, 2010. Tides Online. http://tidesonline.nos.noaa.gov/.

Sonu, C.J., 1968. Collective movement of sediment in littoral environment. *In: Proceedings 11th Coastal Engineering Conference* (Reston, Virginia: ASCE Press), pp. 373–398.

U.S. Army Corps of Engineers, 2010. Wave Information Studies. http://frf.usace.army.mil/wis2010/wis.shtml

U.S. Army Corps of Engineers, 2011. Coastal Inlets Research Program. http://cirp.usace.army.mil/databases/inletsdb/inletsdbinfo.html.

Vincent, C.L. and Corson, W.D., 1981. Geometry of tidal inlets: empirical equations. *Journal of Waterway, Port, Coastal and Ocean Division*, 107(1), 1–9.

Walton, T.L. and Adams, W.D., 1976. Capacity of inlet outer bars to store sand. *In: Proceedings 15th Coastal Engineering Conference* (Reston, Virginia: ASCE Press), pp. 1919–1937.